JCI insight

RESEARCH ARTICLE

Experimental lupus is aggravated in mouse strains with impaired induction of neutrophil extracellular traps

Deborah Kienhöfer,[1] Jonas Hahn,[1] Julia Stoof,[1] Janka Zsófia Csepregi,[2] Christiane Reinwald,[1] Vilma Urbonaviciute,[3] Caroline Johnsson,[4] Christian Maueröder,[1] Malgorzata J. Podolska,[1] Mona H. Biermann,[1] Moritz Leppkes,[5] Thomas Harrer,[1] Malin Hultqvist,[4] Peter Olofsson,[6] Luis E. Munoz,[1] Attila Mocsai,[2] Martin Herrmann,[1] Georg Schett,[1] Rikard Holmdahl,[2] and Markus H. Hoffmann[1]

[1]Friedrich-Alexander-University Erlangen-Nürnberg (FAU), Department of Internal Medicine 3 – Rheumatology and Immunology, Universitätsklinikum Erlangen, Erlangen, Germany. [2]Friedrich-Alexander-University Erlangen-Nürnberg (FAU), Department of Internal Medicine 1 – Gastroenterology, Pneumology and Endocrinology, Universitätsklinikum Erlangen, Erlangen, Germany. [3]Section of Medical Inflammation Research, Department of Medical Biochemistry and Biophysics, Karolinska Institute, Stockholm, Sweden. [4]Redoxis AB, Medicon Village Lund, Sweden. [5]Department of Medicine 1, University of Erlangen-Nuremberg, Erlangen, Germany. [6]ProNoxis AB, Medicon Village Lund, Sweden.

Many effector mechanisms of neutrophils have been implicated in the pathogenesis of systemic lupus erythematosus (SLE). Neutrophil extracellular traps (NETs) have been assigned a particularly detrimental role. Here we investigated the functional impact of neutrophils and NETs on a mouse model of lupus triggered by intraperitoneal injection of the cell death–inducing alkane pristane. Pristane-induced lupus (PIL) was aggravated in 2 mouse strains with impaired induction of NET formation, i.e., NOX2-deficient (*Ncf1*-mutated) and peptidyl arginine deiminase 4–deficient (PAD4-deficient) mice, as seen from elevated levels of antinuclear autoantibodies (ANAs) and exacerbated glomerulonephritis. We observed a dramatically reduced ability to form pristane-induced NETs in vivo in both *Ncf1*-mutated and PAD4-deficient mice, accompanied by higher levels of inflammatory mediators in the peritoneum. Similarly, neutropenic Mcl-1$^{\Delta Myelo}$ mice exhibited higher levels of ANAs, which indicates a regulatory function in lupus of NETs and neutrophils. Blood neutrophils from *Ncf1*-mutated and human individuals with SLE exhibited exuberant spontaneous NET formation. Treatment with specific chemical NOX2 activators induced NET formation and ameliorated PIL. Our findings suggest that aberrant NET is one of the factors promoting experimental lupus-like autoimmunity by uncontrolled release of inflammatory mediators.

Authorship note: D. Kienhöfer and J. Hahn contributed equally to first authorship.

Conflict of interest: C. Johnsson, M. Hultqvist, and P. Olofsson are working for small companies, Redoxis AB and ProNoxis AB, aiming at the development of treatments that use activators of the NOX2 complex. R. Holmdahl and P. Olofsson are cofounders of Redoxis AB and ProNoxis AB. All other authors declare no conflict of interest.

Submitted: January 19, 2017
Accepted: April 10, 2017
Published: May 18, 2017

Reference information:
JCI Insight. 2017;2(10):e92920. https://doi.org/10.1172/jci.insight.92920.

Introduction

Systemic lupus erythematosus (SLE) is a severe autoimmune disease with a prevalence of 0.04% to 0.2%, often affecting women during their child-bearing age. SLE causes systemic inflammation affecting vital organs such as the kidneys, lung, and brain. It is characterized by autoantibodies directed against components of the cell's nucleus. Autoantibodies against autologous nuclear autoantigens play a direct role in SLE's effects on organs, as deposition of immune complexes triggers the production of type I interferons leading to tissue damage (1).

It is thought that the immune system in lupus is sensitized to intracellular antigens following insufficient removal of dead cells, which may either be due to an increase in the rate of cell death which overwhelms the clearance machinery, or due to deficiencies in specific clearance mechanisms such as the complement system (2). As timely clearance fails, the accessibility of nuclear material for the immune system increases and it elicits immune activation and inflammation owing to its function as an alarmin.

Neutrophils are considered an important cell type in the pathogenesis of lupus. These cells are capable of extruding decondensed chromatin decorated with antimicrobial proteins as neutrophil extracellular traps (NETs) to immobilize and kill pathogens (3). Large amounts of antigens from neutrophils may therefore be exposed during acute inflammation. NETs have been implicated as a potential source of autoantigens

in SLE and are therefore prime candidates for the initiation or enhancement of autoimmunity and organ damage. SLE patients produce autoantibodies against a range of nuclear antigens associated with NETs, including double-stranded DNA (dsDNA), histones, and antimicrobial peptides (4, 5), and patients with defective NET degradation show higher levels of anti-NET and anti-dsDNA autoantibodies and develop renal damage (6).

Depending on the stimulating agent, NET formation may depend on production of reactive oxygen species (ROS) during the oxidative burst and on chromatin decondensation mediated by the enzyme peptidylarginine deiminase 4 (PAD4) (7, 8). It could be inferred that deficiency in NETs might reduce the amount of immunogenic nuclear autoantigens. However, it has been observed that *Ncf1*-mutated mice impaired in ROS production due to a deficiency in the NADPH oxidase complex 2 (NOX2) spontaneously develop signs of lupus (9), and NOX2-knockout mice exhibit exacerbated experimental lupus rather than being protected (10). This phenotype included elevated autoantibody production and exacerbated glomerulonephritis. In line with that, a mutation in the NOX2 regulator *NCF2* that causes an approximately 50% decrease in the production of ROS confers an increased risk for developing lupus in humans (11). In addition, humans with chronic granulomatous disease (CGD), who are impaired in the production of ROS and therefore do not undergo classical NET formation are prone to developing lupus-like autoimmunity (12). However, these studies did not investigate the underlying functional mechanisms of the dampening effect of ROS on lupus. The role of neutrophils and NETs in the pathogenesis of lupus therefore needs further elucidation.

Here, we addressed this issue in a lupus mouse model that relies on the alkane pristane (2,6,10,14-tetramethyl-pentadecane). When injected into the peritoneal cavity, the naturally occurring hydrocarbon oil pristane induces chronic peritonitis accompanied by production of autoantibodies directed against DNA- and RNA-associated autoantigens and chronic inflammation, resulting in a disease closely resembling and meeting the classification criteria of SLE (13–16). Susceptibility to pristane-induced lupus (PIL) shows a female prevalence and is widespread among commonly used mouse strains, with diverse kinds of organ manifestation depending on the genetic background (17, 18). In BALB/c mice, pristane prompts immune complex–mediated glomerulonephritis (19), whereas mice on the C57BL/6 background develop comparably mild kidney disease but instead contract a diffuse alveolar hemorrhage resembling the serious complication seen in a subgroup of patients with SLE (20, 21). Furthermore, pristane triggers NET formation, apoptosis, and necrosis (22, 23). Of note, environmental exposure to pristane is also associated with development of SLE in humans (24). PIL is therefore an ideal model to investigate the implication of NETs in the development of lupus-like autoimmunity.

We show that PIL is exacerbated in a neutrophil-deficient mouse strain (Mcl1$^{\Delta Myelo}$ mice). Similarly, 2 mouse strains with normal neutrophil numbers but impaired pristane-induced NET formation (*Ncf1*** and PAD4$^{-/-}$ mice) developed aggravated PIL accompanied by increased levels of lupus autoantibodies and exacerbated renal damage. In contrast, treatment with a NOX2-activating agent that triggers NET formation dampened autoantibody production and ameliorated lupus-associated glomerulonephritis. This study provides evidence that NOX2- and PAD4-mediated generation of NETs is needed to control autoimmunity and organ damage in PIL.

Results

Increased antinuclear antibody levels in the absence of neutrophils. Neutrophils have been implicated in both the development and regulation of inflammatory and autoimmune disorders, but their net influence on lupus-like autoimmunity has not been investigated. While depletion of neutrophils can be performed by injection of specific antibodies (anti-Gr1 or anti-Ly6G), such a strategy is not feasible over the extended period that PIL needs to develop. We therefore used mice with a myeloid-specific conditional deletion of the antiapoptotic protein Mcl-1 (LysM$^{Cre/Cre}$ Mcl-1$^{fl/fl}$ mutants, referred to as Mcl-1$^{\Delta Myelo}$ mice), which exhibit a selective neutrophil deficiency caused by the requirement of Mcl-1 for the survival of neutrophils, whereas other myeloid-lineage cells are not affected (ref. 25 and J.Z.C. and A.M., unpublished observations). Mcl-1$^{\Delta Myelo}$ mice were not protected from lupus but instead exhibited strongly exacerbated IgG anti-dsDNA, anti-Sm/RNP, and anti-histone autoantibody levels even in the absence of pristane injection (Figure 1A), accompanied by higher serum cytokine concentrations (Figure 1C). In contrast, proteinuria caused by PIL was not different between Mcl-1$^{\Delta Myelo}$ and control mice (Figure 1B). Thus, the presence of functional neutrophils in the periphery seems to be dispensable for autoantibody production but not glomerular damage in PIL.

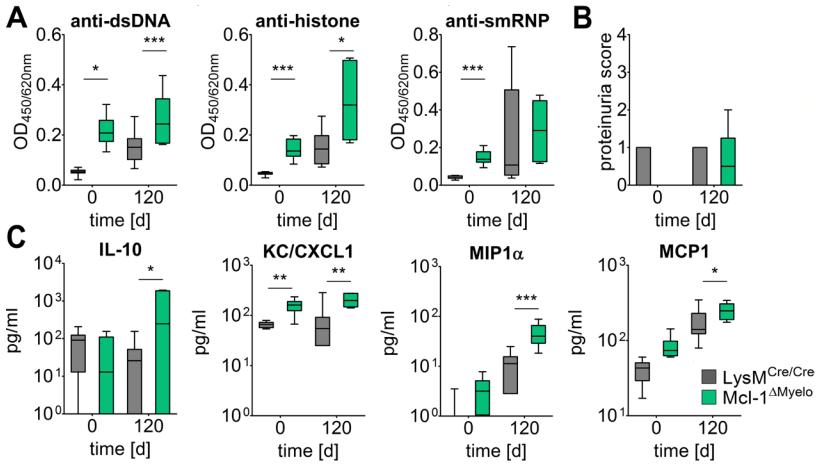

Figure 1. Influence of neutrophils on pristane-induced lupus. (**A**) Levels of autoantibodies against double-stranded DNA (dsDNA), histone, and Sm/RNP, and (**B**) proteinuria in neutrophil-deficient Mcl-1$^{\Delta Myelo}$ and LysM$^{Cre/Cre}$ control mice before and 120 days after pristane injection. (**C**) Serum levels of selected cytokines and chemokines in Mcl-1$^{\Delta Myelo}$ and LysM$^{Cre/Cre}$ mice before and 120 days after pristane injection. In all panels, boundaries of boxes represent 25th/75th percentiles, lines within boxes indicate medians, and whiskers represent minimum/maximum values for 6 to 10 animals in each cohort. $^{*}P < 0.05$, $^{**}P < 0.01$, $^{***}P < 0.001$, as determined by 2-way ANOVA with Bonferroni's post-hoc test.

Deficiency of ROS results in exacerbated experimental lupus characterized by higher autoantibody production and more severe renal disease. Naive BALB/c.*Ncf1*** mice carry a mutation in one of the regulatory subunits of the NOX2 complex that completely inhibits ROS production by NOX2. This autoimmune-prone mouse strain is characterized by spontaneous production of low levels of typical lupus autoantibodies and deposition of IgG and complement factor C3 in the renal glomeruli (9). Pristane-primed production of lupus autoantibodies was dramatically increased in BALB/c.*Ncf1*** mice as compared with their WT littermates (Figure 2A). Several IgG anti-dsDNA subtypes were significantly increased in BALB/c.*Ncf1*** mice, with the strongest effect seen in IgG1 and IgG2a production (Figure 2B), suggesting that lupus autoantibodies were mainly derived from class-switched B cells. In contrast, production of IgG2b and IgM anti-dsDNA autoantibodies was not significantly different in *Ncf1*** and WT mice. These results are in line with reports from NOX2-deficient MRL^{lpr} mice that had higher numbers of IgG2a but not IgM antibody–forming cells (10).

In concert with the higher autoantibody production, *Ncf1*** mice exhibited strongly enhanced and accelerated deposition of IgG and complement factor C3 in their glomeruli (Figure 2C and Supplemental Figure 1A; supplemental material available online with this article; https://doi.org/10.1172/jci.insight.92920DS1). Histological analysis of the kidneys revealed enlarged hypercellular glomeruli in pristane-injected animals, with complete loss of glomerular architecture in *Ncf1*** as compared with WT animals (Figure 2D). This process was accompanied by exacerbated proteinuria and premature death in *Ncf1*** mice (Figure 2E and Supplemental Figure 1B).

The more severe disease course in *Ncf1*** mice was mirrored by higher plasma levels of inflammatory cytokines and chemokines, for example IL-12, IL-6, or MCP-1 (Figure 2F). Along with type I IFNs and IFN-γ, IL-12 and IL-6 promote autoantibody production in PIL. IL-12 also mediates structural renal damage after renal immune complex deposition (26).

The IFN signature that is typical for PIL and SLE was also enhanced in *Ncf1*** mice (Supplemental Figure 1C). Although IFN-α protein was not detectable in sera, expression of IFN-α mRNA was significantly higher in blood cells of unchallenged *Ncf1*** as compared with WT mice.

Pristane-induced NET formation depends on functional NOX2 and PAD4 and regulates the concentration of inflammatory mediators. Next we investigated whether pristane induces NET formation in the peritoneum and if this property is maintained in *Ncf1*** mice. In line with previous reports (27), pristane injection led to an influx of various phagocyte subsets into the peritoneum. The cellular compositions of the infiltrates 2 weeks after pristane injection were similar in *Ncf1*** and WT mice (Figure 3A), showing that the migratory capacity of phagocytes into the peritoneum is not impaired in the absence of ROS.

The citrullination of histones has been widely used to distinguish NETs from other forms of cell death (28), although not all NET inducers trigger histone citrullination (29). Pristane did elicit the formation of citrullinated histone H3–positive (citH3^{+}) cells with extracellular DNA (NETs) in the peritonea of WT mice, whereas their numbers were drastically reduced in the peritonea of *Ncf1*** mice. This result shows that pristane-induced NET formation is dependent on NOX2-derived ROS in vivo (Figure 3, B and C).

Serine proteases bound to NETs have been shown to degrade cytokines and chemokines, which contributes to a dampening of arthritis induced by injection of monosodium urate crystals or zymosan (30, 31). This mechanism could also influence other forms of inflammatory diseases where neutrophils play

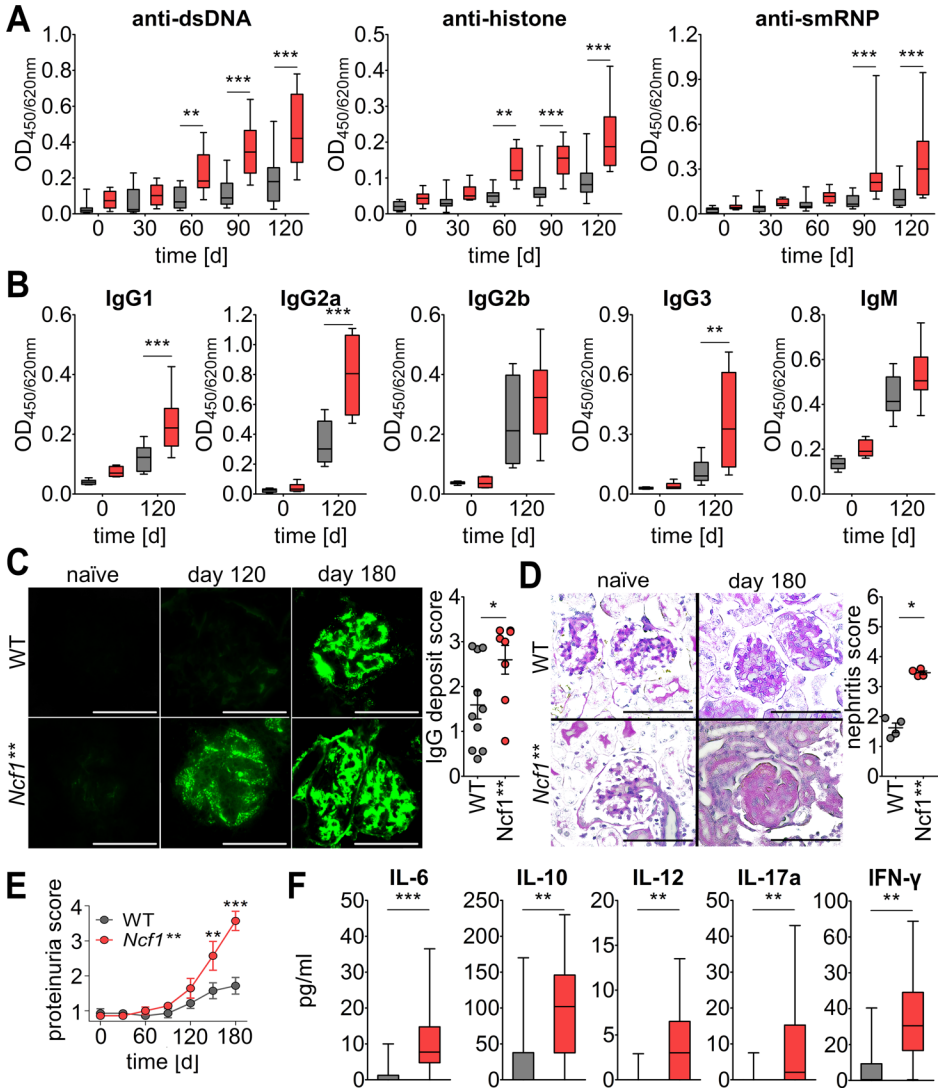

Figure 2. Exacerbated pristane-induced lupus in the absence of NOX2-derived ROS. (**A**) BALB/c.*Ncf1*** mice produce higher levels of lupus autoantibodies and develop aggravated renal damage. IgG autoantibodies against double-stranded DNA (dsDNA), Sm/RNP, and histone were analyzed in sera of naive and pristane-primed mice (n = 13) by ELISA. Boundaries of boxes represent 25th/75th percentiles, lines within boxes indicate medians, and whiskers represent minimum/maximum values. Significant differences after testing by 2-way ANOVA with Bonferroni's post-hoc test were detected beginning 60 days after pristane injection. (**B**) Box-and-whisker plots of IgG1, IgG2a, IgG2b, IgG3, and IgM anti-dsDNA autoantibodies in sera of pristane-injected BALB/c.*Ncf1*** and BALB/c WT mice (n = 8). $^{**}P < 0.01$, $^{***}P < 0.001$, as determined by 2-way ANOVA with Bonferroni's post-hoc test. (**C**) Representative immunofluorescence images of renal IgG deposits in BALB/c WT and BALB/c.*Ncf1*** mice before and 4 and 6 months after pristane injection. Scale bars: 100 μm. Scatter plot shows individual values, mean, and SEM of deposits at day 180 from 8 to 10 mice. $^{*}P < 0.05$ as determined by 2-tailed Student's t test. (**D**) Representative periodic acid–Schiff staining of kidneys from unchallenged and pristane-injected BALB/c WT and *Ncf1*** mice. Dramatically worsened mesangial cell and matrix expansion at day 180 after pristane injection can be seen in BALB/c.*Ncf1*** mice. Scale bars: 100 μm. Scatter plot shows individual values, mean, and SEM of renal damage at day 180 (n = 4). $^{*}P < 0.05$ as determined by 2-tailed Student's t test. (**E**) Monthly quantification of proteinuria in BALB/c.*Ncf1*** and WT mice before and after pristane injection. Shown are means and SEM (n = 7). $^{**}P < 0.01$, $^{***}P < 0.001$, as determined by 2-way ANOVA using Bonferroni's post-hoc test. (**F**) Box-and-whisker plots showing medians, 25th/75th percentiles, and minimum/maximum values of serum cytokine/chemokine concentrations from mice 3 months after pristane injection (n = 14). $^{**}P < 0.01$, $^{***}P < 0.001$ as determined by 2-tailed Mann-Whitney U test.

a role, e.g., lupus. In support of this, we found the peritoneal concentrations of inflammatory mediators such as TNF-α and IL-6 to be elevated in the relative absence of NETs in *Ncf1*** mice (Figure 3D), whereas the concentrations of the chemokine KC/CXCL1, which was previously shown to be released in large amounts from NETs (30), were not significantly different. Thus, deficiency in NET formation is associated with elevated levels of proinflammatory mediators.

Pristane-induced NET formation is strongly inhibited in *Ncf1*** mice. However, we found an elevated percentage of cells having undergone chromatin decondensation in blood cells of naive *Ncf1*** mice (Figure

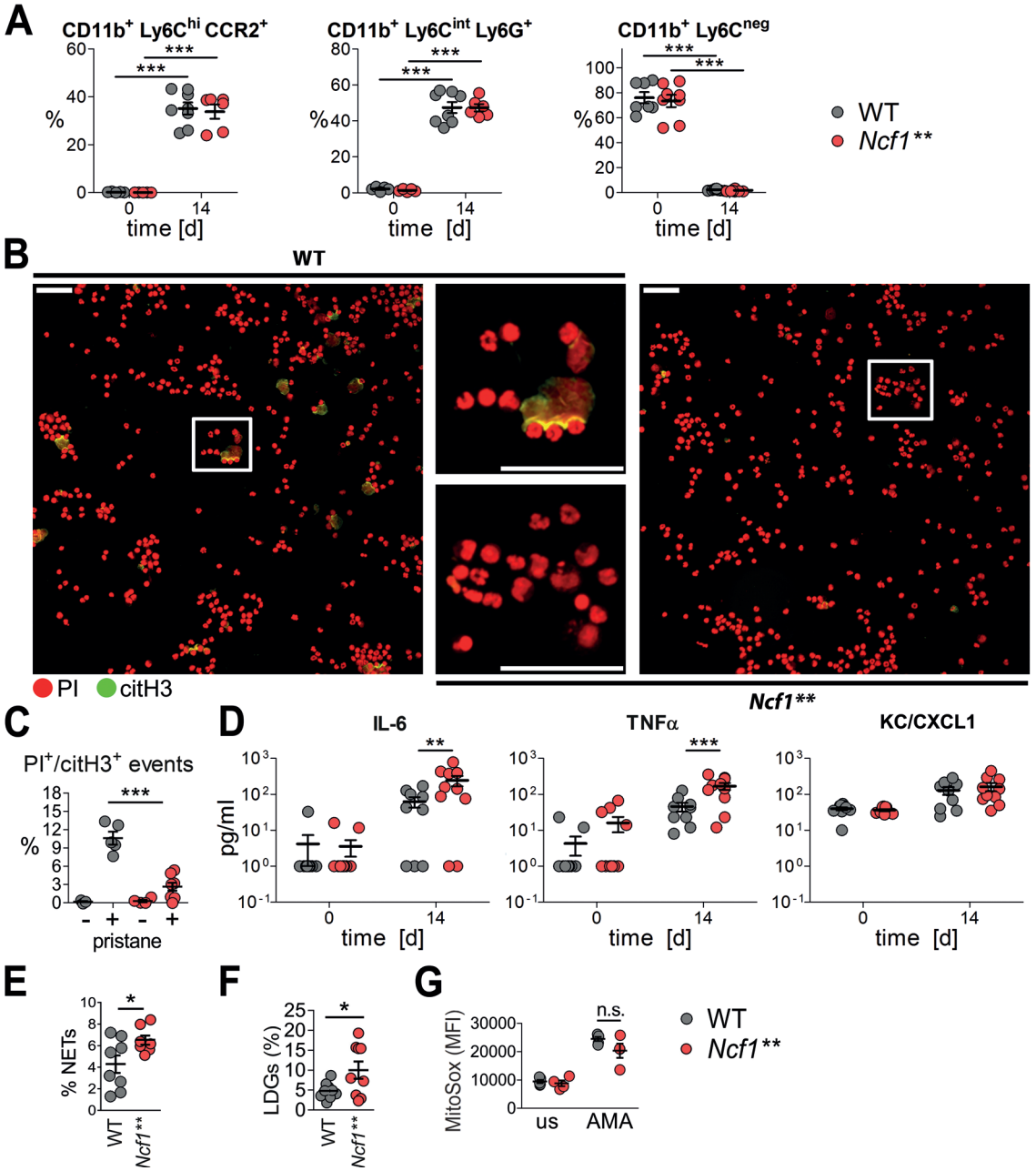

Figure 3. Impaired pristane-induced but enhanced spontaneous neutrophil extracellular trap (NET) formation in *Ncf1* mice.** (**A**) Percentages of CD11b$^+$Ly6C^{hi}CCR2$^+$ monocytes, CD11b$^+$Ly6C^{int}Ly6G$^+$ neutrophils, and CD11b$^+$Ly6C$^-$ cells in the peritonea of BALB/c.*Ncf1*** and WT mice before and 14 days after injection of pristane. Scatter plots show individual values, means, and SEM (n = 5–8). ***$P < 0.001$ as determined by ANOVA with Bonferroni post-hoc test. (**B**) Representative fluorescence microscopy images and (**C**) quantification of peritoneal cells isolated 1 day after injection of pristane and stained for DNA with propidium iodide (PI, red) and for citrullinated histone H3 (citH3, green). Scale bars: 100 μm. Scatter plot shows individual values, means, and SEM (n = 4–8). PI$^+$citH3$^+$ events represent cells having undergone NETosis. ***$P < 0.001$ as determined by ANOVA with Bonferroni post-hoc test. (**D**) Concentrations of selected cytokines and chemokines in peritoneal lavages of BALB/c.*Ncf1*** and WT mice 0 and 14 days after injection of pristane. Scatter plot shows individual values, means, and SEM (n = 10). **$P < 0.01$, ***$P < 0.001$ as determined by ANOVA with Bonferroni post-hoc test. (**E**) Quantitative analysis of NETing cells in blood drawn from untreated BALB/c WT and *Ncf1*** mice. Scatter plot shows individual values, mean, and SEM of percentages of cells having undergone NET formation (PI$^+$citH3$^+$ events) in 7 to 8 mice. *$P < 0.05$ as determined by 2-tailed Student's t test. (**F**) Percentage of CD11b$^+$Ly6C^{int} Ly6G$^+$ cells in the peripheral blood mononuclear cell fraction after density gradient centrifugation performed on blood of BALB/c WT and *Ncf1*** mice. Scatter plot shows individual values, mean, and SEM, n = 9. *$P < 0.05$ as determined by 2-tailed Student's t test using Welch's correction for unequal variances. LDG, low-density granulocyte. (**G**) Spontaneous and antimycin A–induced (AMA-induced) mitochondrial ROS production (MitoSOX mean fluorescence intensity [MFI]) in BALB/c WT and *Ncf1*** mice. Scatter plots show individual values, means, and SEM of 4 to 5 animals. n.s., not significant.

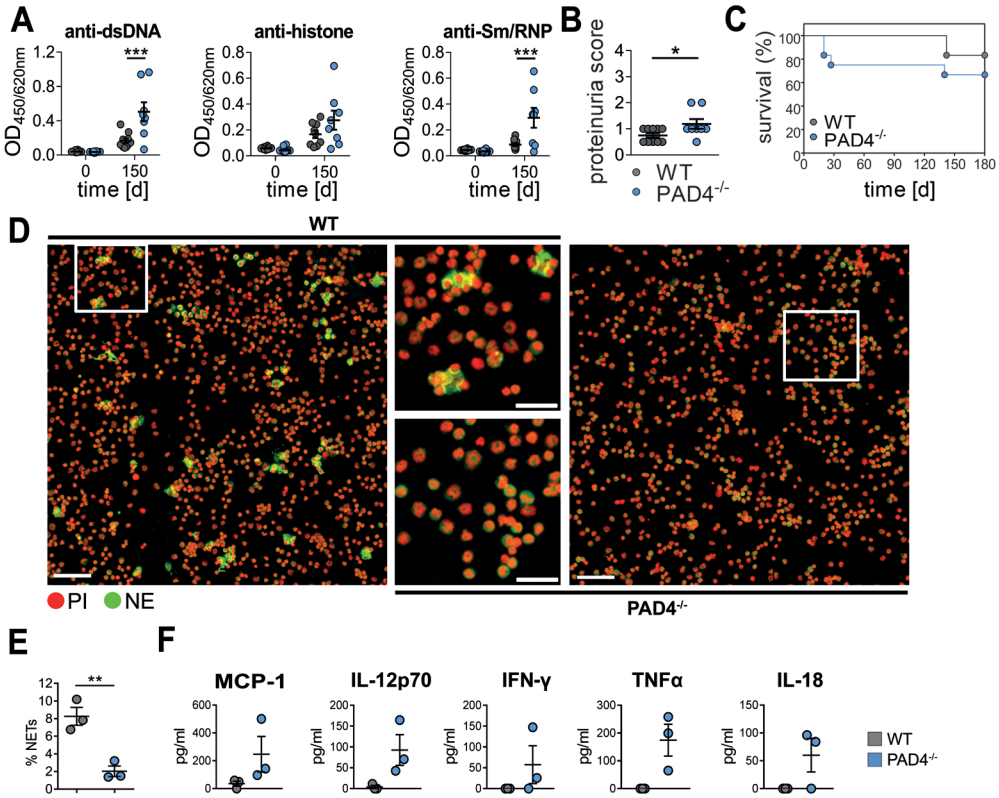

Figure 4. Exacerbated pristane-induced lupus in NET-deficient PAD4$^{-/-}$ mice. (**A**) Development of lupus autoantibodies in C57BL/6 WT and PAD4$^{-/-}$ mice. Autoantibodies against double-stranded DNA (dsDNA), Sm/RNP, and histone were analyzed in sera of naive mice and mice 150 days after pristane priming by ELISA. Scatter plots show individual measurements, means, and SEM of 8 to 12 mice per group. ***$P < 0.001$ as determined by 2-way ANOVA with Bonferroni post-hoc test. (**B**) Quantification of proteinuria in C57BL/6 WT and PAD4$^{-/-}$ mice 150 days after pristane injection ($n = 8$). *$P < 0.05$ as determined by 2-tailed Student's *t* test. (**C**) Survival plot of C57BL/6 WT and PAD4$^{-/-}$ mice after pristane injection ($n = 12$). (**D**) Representative fluorescence microscopy images and (**E**) quantification of peritoneal cells isolated 1 day after injection of pristane from PAD4$^{-/-}$ and WT mice and stained for DNA with propidium iodide (PI, red) and for neutrophil elastase (NE, green). Scale bars: 100 μm. Scatter plot in **E** shows individual values, mean, and SEM of cells having undergone neutrophil extracellular trap (NET) formation, defined as PI$^+$NE$^+$ events with a 5-fold greater mean nuclear size. **$P < 0.01$ as determined by 2-tailed Student's *t* test. (**F**) Concentrations of selected cytokines and chemokines in peritoneal lavages from PAD4$^{-/-}$and WT mice 0 and 1 day after injection of pristane. Scatter plots show individual values, means, and SEM of 3 mice per group.

3E), along with higher percentages of CD11b$^+$Ly6C^{int}Ly6G$^+$ low-density granulocytes (LDGs) (Figure 3F), a distinct proinflammatory neutrophil subset that was proposed to have a detrimental role in SLE, owing to a higher production of inflammatory cytokines, enhanced tissue damaging properties, and higher levels of spontaneous NET formation (32–34). A recent study has shown that elevated spontaneous formation of NETs in the absence of NOX-derived ROS in individuals with CGD is driven by ROS from mitochondria (35). To elucidate if production of mitochondrial ROS is differentially regulated in *Ncf1*** mice, we used MitoSOX, a red fluorescent dye used for specific detection of mitochondrial superoxide in live cells. Triggering of spontaneous or antimycin A–induced production of mitochondrial ROS was not significantly different between *Ncf1*** and WT mice (Figure 3G).

Neutrophils make use of ROS and/or histone citrullination by PAD4 in contact with biochemical and particulate stimuli while extruding NETs (7, 8). To confirm the specific role of NETs in lupus, we conducted PIL in mice deficient for PAD4. In accordance with results from *Ncf1*** mice, autoantibody levels and proteinuria after injection of pristane were higher in PAD4-deficient mice (Figure 4, A and B). Pristane-induced renal damage is generally less dramatic on the C57BL/6 background, and thus survival rates were not significantly different (Figure 4C). Impaired pristane-induced in vivo NET formation in PAD4-deficient mice was associated with higher peritoneal concentrations of inflammatory mediators after pristane injection (Figure 4, D–F). This phenocopies the effect of ROS deficiency in *Ncf1*** mice and suggests a protective effect of NETs on the severity of PIL.

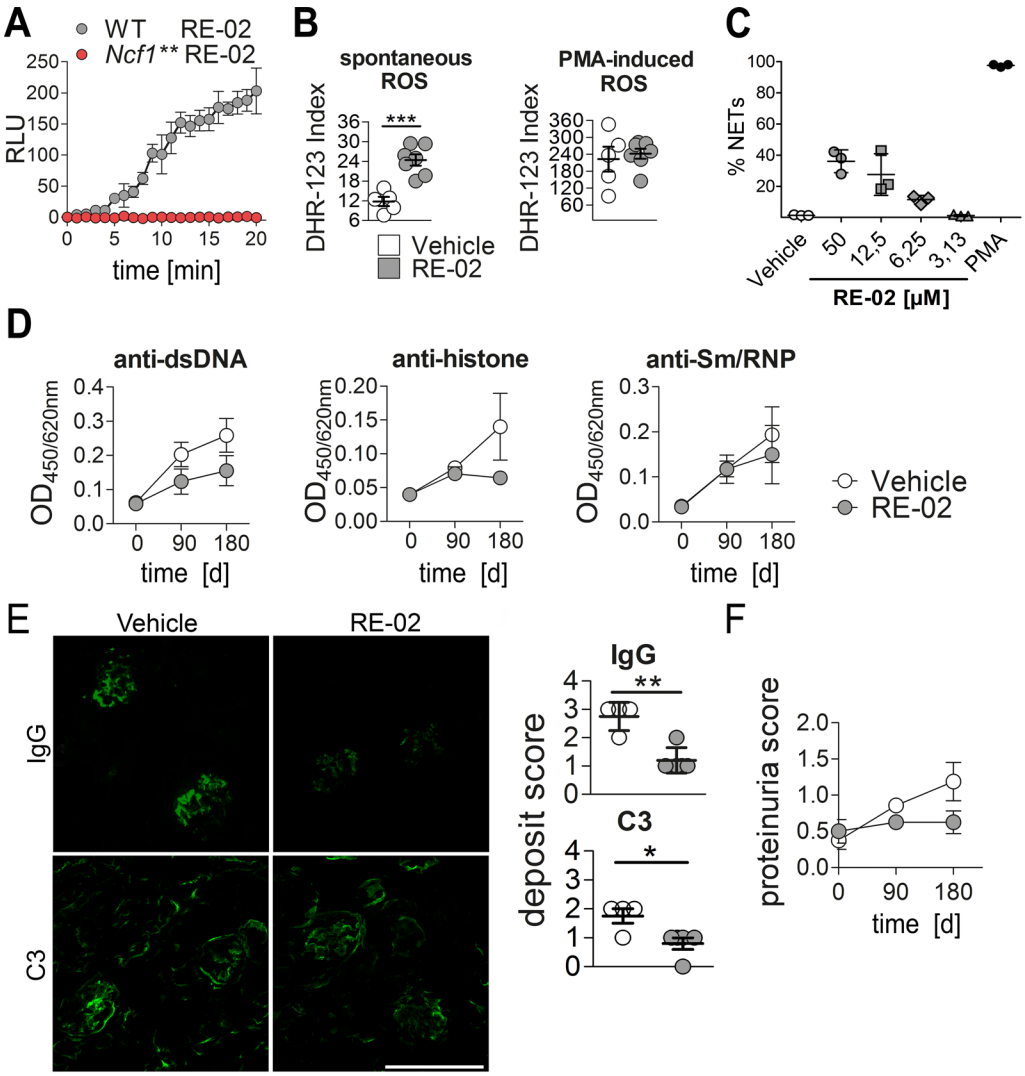

Figure 5. Treatment of pristane-induced lupus (PIL) with a NOX2 agonist. (**A**) Extracellular release of ROS (relative light units, RLU) from peritoneal cells isolated from WT or *Ncf1*** mice and treated with the NOX2 activator RE-02. Background values from vehicle-treated cells are subtracted. Line plots show means and SEM of 4 animals per group. (**B**) ROS production of cells isolated from mice treated s.c. twice weekly for 180 days with RE-02 or vehicle. Scatter plots show individual values, means, and SEM from 8 animals per group. ***$P < 0.001$ as determined by 2-tailed Student's *t* test. (**C**) Quantitative analysis of neutrophil extracellular traps (NETs) in blood neutrophils treated for 3 hours with different concentrations of RE-02 or PMA. NETs were defined as SYTOX Green– and neutrophil elastase–positive (SYTOX Green$^+$NE$^+$) events with a 5-fold greater mean nuclear size. Scatter plot shows individual values, means, and SEM from 3 normal healthy control donors. (**D**) IgG autoantibodies against double-stranded DNA (dsDNA) and Sm/RNP throughout PIL in mice treated with RE-02 or vehicle were analyzed in sera ($n = 8$ per group) by ELISA. Shown are means ± SEM. (**E**) Representative immunofluorescence images of glomerular IgG and complement C3 deposits in mice 180 days after pristane injection that were treated with RE-02 or vehicle. Scale bar: 100 µm. Right panel shows scatter plots of glomerular deposition scores for IgG and complement factor C3. Depicted are individual values, means, and SEM ($n = 4–5$). *$P < 0.05$, **$P < 0.01$ as determined by 2-tailed Student's *t* test. (**F**) Quantification of proteinuria in RE-02– or vehicle-treated mice at day 0, 90, and 180 after pristane injection. Bars show means and SEM ($n = 8$).

Treatment of PIL with activators of ROS production. Our finding that in the absence of NOX2-dependent ROS production PIL is drastically exacerbated prompted us to investigate if enhanced ROS production might protect against PIL in mice with functional NOX2, and thus, if small-molecule activators of NOX2 could be potential candidates for therapeutic drugs. In order to investigate if activation of ROS production can ameliorate lupus we used the newly developed specific NOX2 activator RE-02 (Redoxis AB). In cells isolated from the peritonea of thioglycollate-injected C57BL/10.Q WT mice, compound RE-02 confirmedly increased extracellular ROS production. In contrast, no ROS were released from peritoneal cells of *Ncf1*** mice after treatment with RE-02, confirming that the compound specifically targets NOX2 (Figure 5A). We then treated PIL by twice weekly subcutaneous injection of RE-02 and determined ROS production again before euthanizing the mice. Blood cells derived from mice treated with RE-02 produced

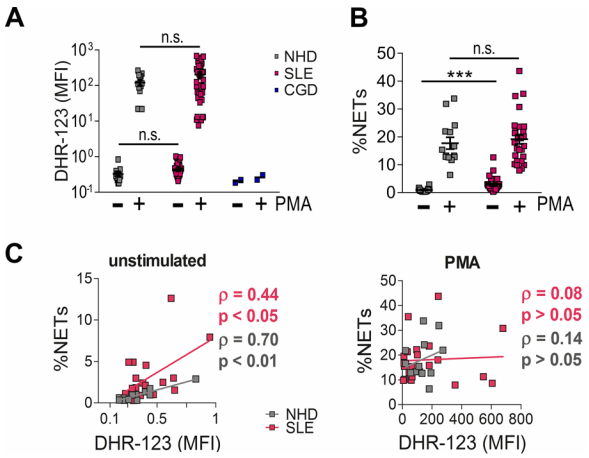

Figure 6. ROS production and neutrophil extracellular trap (NET) formation in human individuals with SLE. (**A**) ROS production in neutrophils from systemic lupus erythematosus (SLE) patients and normal healthy donors (NHDs). The capacities of $CD14^{-}CD16^{+}$ polymorphonuclear leukocytes (PMNs) from NHDs (n = 13), SLE patients (n = 34), and patients with chronic granulomatous disease (CGD, n = 2), to produce ROS spontaneously or upon activation with PMA were investigated using flow cytometry. Scatter plots show individual values, means, and SEM of dihydrorhodamine 123 (DHR-123) mean fluorescence intensity (MFI). n.s., not significant, as determined by Kruskal-Wallis test using Dunn's multiple comparison test. (**B**) Quantitative analysis of NETing cells in whole blood drawn from individuals with SLE and NHDs. Scatter plots show individual values, means, and SEM of percentages of propidium iodide– and neutrophil elastase–positive ($PI^{+}NE^{+}$) events with a 5-fold greater mean nuclear size; n = 24 (NHDs) or n = 27 (SLE). ***P < 0.001, n.s., not significant, as determined by Kruskal-Wallis test using Dunn's test for multiple comparison. (**C**) Correlation analysis between ROS production and spontaneous and PMA-induced NET formation in PMNs from SLE patients and NHDs. Spearman coefficients (ρ) and P values (determined by 2-tailed Student's t test) are depicted within the graphs.

more spontaneous ROS than cells from vehicle-treated animals, whereas PMA-induced ROS production was not different (Figure 5B). Treatment of blood neutrophils with RE-02 triggered chromatin decondensation and the formation of NETs in a concentration-dependent manner (Figure 5C). Importantly, the NOX2 activator RE-02 showed a strong trend towards ameliorating the development of PIL in WT mice, as seen by decreased autoantibody production (Figure 5D), fewer glomerular deposits (Figure 5E), and less proteinuria (Figure 5F).

ROS production and NET formation in human individuals with SLE. To investigate if our results from PIL translate to humans, we first quantified ROS production by flow cytometry in a cohort of 39 individuals fulfilling at least 4 of the classification criteria of SLE (15, 36) and 18 normal healthy donors (NHDs) (Supplemental Table 1). Blood samples from patients with CGD served as negative controls (Figure 6A). In contrast to a previous study (37), we did not find differences in ROS production from granulocytes of NHDs and SLE patients with our methodology.

We then analyzed the in vitro capacity to undergo NET formation in isolated blood neutrophils from SLE patients and NHDs. Neutrophils from individuals with SLE and NHD were incubated with or without the known NETosis inducer PMA. We then quantified NETs by fluorescence microscopy and morphometry. In line with published data (32), spontaneous NET formation was higher in SLE patients than in healthy controls (Figure 6B), whereas PMA-induced NETosis was not. Spontaneous but not PMA-induced ROS production from SLE and NHD granulocytes correlated with the amount of NETs (Figure 6C).

Discussion

Neutrophils, the immune system's first line of defense, follow 3 main effector pathways in the response to inflammatory stimuli, i.e., phagocytosis of the insulting organism or agent, expulsion of granular content, and extrusion of a meshwork of DNA decorated with antimicrobial molecules and proteinases (NETs). Many aspects of neutrophil biology have been implicated in the development and regulation of lupus (38). In the majority of these reports, neutrophils were assigned the role of a villain that fuels aberrant immune responses and causes tissue damage. This role is supported by the encouraging results of studies using PAD4 inhibitors in lupus and other autoinflammatory conditions (39–42).

Our data from neutropenic Mcl-$1^{\Delta Myelo}$ mice indicate that neutrophils can also serve important regulatory cell functions in lupus-like autoimmunity. In Mcl-$1^{\Delta Myelo}$ mice, survival of neutrophils is severely impaired due to a knockout of the antiapoptotic protein Mcl-1. These mice have elevated numbers of apoptotic and secondary necrotic neutrophils in their bone marrow and blood that might serve as a source of nuclear autoantigens, which might explain the higher titers of antinuclear antibodies (ANAs) seen in Mcl-$1^{\Delta Myelo}$ mice also in the absence of pristane injection. Nevertheless, our results from this strain show that lupus occurs also in the absence of neutrophils. The peculiar phenotype seen in this neutrophil-deficient mouse strain together with our results from *Ncf1*** and $PAD4^{-/-}$ mice therefore reveal that neutrophils and NETs are not necessarily driving all kinds of lupus-like autoimmunity.

The NOX2 complex is predominantly expressed in phagocytes and is the dominant ROS-generating complex in mammals (43). ROS production via NOX2 is regulated by the cytosolic adaptors $p47^{phox}$ (Ncf1)

and p40^{phox} (Ncf4) that bridge interactions of NOX activators with the enzymatic flavocytochrome components embedded in phagosomal and plasma membranes.

A strong correlation between a low capacity to produce NOX2-derived ROS and autoimmune disease is known from rodent models of arthritis (44, 45), multiple sclerosis (45), psoriasis (46), and Guillain-Barre syndrome (47). An increased inflammatory response in the absence of ROS has also been observed in conditions that are not considered classical autoimmune diseases, for example in zymosan- or monosodium urate crystal–induced inflammation (30, 48, 49). This indicates that ROS also regulates T cell–independent inflammatory pathways.

A dampening effect of NOX2 on murine lupus was previously reported in a NOX2-deficient mouse strain crossed with MRL.*Fas*^{lpr} mice (10). However, a complete genetic deficiency of the NOX2 complex is not commonly found in humans. Instead, various mutations in *NCF1* are linked to CGD (50). We therefore employed a mouse strain carrying a naturally occurring mutation in *Ncf1* that abrogates NOX2-dependent ROS production. Using these *Ncf1*** mice we tested the influence of NOX2-derived ROS in a mouse model of lupus induced by intraperitoneal injection of the alkane oil pristane. Current concepts envisage that autoreactivity in PIL follows massive cell infiltration accompanied by cell death in the peritoneum after pristane injection and causing an overload of the clearance machinery (51). We aimed to shed light on the role of ROS and especially NETs in the etiopathogenesis of murine lupus by examining PIL in *Ncf1*** mice.

*Ncf1*** mice developed significantly elevated levels of ANAs, exemplified by antibodies against dsDNA, histones, and Sm/RNP. These autoantibody subsets are very specific to SLE and are associated with disease severity and organ damage (52–54). In line with that, *Ncf1*** mice with PIL suffered exacerbated glomerulonephritis and died earlier than their WT littermates.

Apart from degradation of proinflammatory mediators by NET-bound proteases (30, 31) there are several other ways that the oxidative burst in phagocytes could influence lupus. NOX2 supports the function of T regulatory cells and changes the activation threshold of autoreactive T cells; it influences protein phosphatases, protein tyrosine kinases, the linker for activation of T cells (LAT), and tryptophan metabolism/IDO; regulates the IFN/STAT1 pathway and innate lymphocyte activation; and contributes to regulation of autophagy, although some of these suggested mechanism are controversial (reviewed in ref. 55).

To specifically assess the relative impact of NETs we used PAD4$^{-/-}$ mice that have functional NOX2 yet are unable to form NETs in response to calcium-dependent signals. In a study by Knight et al. mice treated with Cl-Amidine, an inhibitor of all PAD enzymes, exhibited increased levels of autoantibodies but decreased glomerular deposition (39). In line with these findings, we observed a stronger inflammatory response in the peritonea of pristane-challenged PAD4$^{-/-}$ mice, which was associated with higher levels of ANA, whereas glomerular deposition was on a very low level in both WT and PAD$^{-/-}$ animals, which is typical for PIL in mice on the C57BL/6 background. However, the PAD4$^{-/-}$ mice developed significantly higher proteinuria than their WT counterparts. It might be that suppression of other PAD enzymes in Cl-Amidine–treated mice or the different disease mechanism in the utilized mouse model can account for those different observations.

We propose a concept in which PIL is influenced by NET formation that is dependent on both ROS and PAD4 (Supplemental Figure 2). In PIL, pristane triggers various forms of cell death in the peritoneum and the corpses of these cells cannot be removed quickly enough to prevent antinuclear autoreactivity and chronic release of proinflammatory mediators. In the absence of NETs the degradation of the arising proinflammatory mediators is impaired. Since ROS production by NOX2 in neutrophils also occurs intracellularly, NET formation might also constitute a mechanism to release ROS, endowing its antiinflammatory action on other cell types.

Of note, a lively discussion is currently ongoing about key aspects of NETs, their contents and morphology (56), how their formation should be precisely named to reflect the different pathways of their generation (29, 57), and the fate of the NETing neutrophil (58). It is not the primary aim of our study to fundamentally contribute to this discussion. Instead, we focus on the clinical aspects of extracellular DNA bound to neutrophil-derived proteases (denominated here as NETs).

Interestingly, the NET-inducing NOX2 activator RE-02 ameliorated PIL. This small molecule was selected from a high-throughput screening for capacity to induce NOX2-derived ROS release in a human neutrophil–like cell line and in fresh rat phagocytes (59). Selected compounds from this screen were then validated for their ROS-inducing capacity and one lead molecule, the sulfonamide compound RE-02, was selected for treatment of PIL. Therapeutic intervention by NOX2 activators might shift the balance towards

resolution of inflammation by promoting inflammatory cytokine degradation in NETs. It will be interesting to determine whether the NOX2 activator RE-02 just interferes with the initial events of autoimmunity or whether it is still effective in fully developed disease when high levels of ANAs have already formed. Future studies will therefore also apply therapeutic settings for the treatment of PIL and other lupus models. Furthermore, by RE-02 treatment of PIL in PAD4$^{-/-}$ mice we will investigate whether the effect of RE-02 is mediated mainly through NET formation or if NET-independent effects of ROS on cell signaling play a significant role as well.

While lupus was exacerbated when pristane-induced NET formation was impaired, blood neutrophils from both lupus-prone *Ncf1*** mice and individuals with SLE formed exuberant NETs in the absence of external stimulation. Hence, the relationship between the capacity to form NETs and the severity of lupus appears complex. Whereas increased presence of NETs in the blood in lupus might fuel the inflammatory process, NET formation appears to be an important dampening factor on inflammation in the pristane-injected peritoneal cavity. This may be explained by the different concentrations of neutrophils and NETs in blood and the peritoneum; in low densities in peripheral blood, the proinflammatory roles of NETs predominate, but in a densely infiltrated site of sterile inflammation the degradation of inflammatory mediators in NETs is the preponderant factor (30, 60). Alternatively or in addition, pronounced spontaneous NET formation ex vivo might be a consequence of a disturbed cytokine milieu in established SLE and *Ncf1*** mice.

In conclusion, while not directly challenging the concept of a detrimental role of persistent peripheral NETs in established SLE, our overall results suggest that NETs can also have a protective role against the development of certain forms of lupus, as per example drug-induced lupus. Considering the pending development of therapeutics aiming at inhibiting NET formation for the treatment of lupus in humans, extreme caution needs to be exercised to identify the precise clinical conditions and developmental stages of lupus that warrant the use of such therapeutic agents.

Methods

Mice. Mice with a mutated *Ncf1* (*Ncf*$^{m1j/m1j}$, denoted as *Ncf1***) were kept on BALB/c.Q and C57BL/10.Q backgrounds. The *Ncf1* mutation impairs translocation of the Ncf1 (p47^{phox}) protein to the membrane upon activation, thereby completely blocking function of the NOX2 complex (61, 62). PAD4$^{-/-}$ (provided by Kerri Mowen, Scripps Institute), Mcl-1$^{\Delta Myelo}$, and control mice were on the C57BL/6 genetic background. Experiments were performed on female mice frequency-matched for age, and evaluated with blinded identity.

Experimental peritonitis and lupus. PIL was induced by a single intraperitoneal injection of 500 μl pristane (Sigma-Aldrich) in female mice at 8 to 12 weeks of age and followed over 6 months. Serum was prepared before injection of pristane and in monthly intervals thereafter. To analyze the effect of elevated ROS production on PIL, mice were treated twice weekly by subcutaneous injection of 7 mg/kg of the NOX2 agonist RE-02 (in medium-chain triglyceride oil/10% DMSO/10% ethanol) or with vehicle.

Determination of autoantibodies and serum cytokines. For detection of murine autoantibodies by ELISA, microtiter plates were coated with 50 μg/ml histone from calf thymus (Roche), 1 μg/ml Sm/RNP (GenWay Biotech), or precoated with 20 μg/ml poly-L-lysine (Sigma-Aldrich) before adding 20 μg/ml calf thymus DNA (Sigma-Aldrich). PIL-sera were added at a 1:100 dilution in PBS/2% FCS. Bound IgG or IgM was detected with 0.125 μg/ml horseradish peroxidase–conjugated goat anti–mouse IgG1 (catalog 1072-01), IgG2a (catalog 1082-01), IgG2b (catalog 1092-05), IgG3 (catalog 1102-05), IgG(H+L) (catalog 1020-05), or IgM (catalog 1021-05) (all Southern Biotech) and substrate solution (eBioScience). Human and murine cytokines/ chemokines in sera/plasma and peritoneal lavages were analyzed by Legendplex bead technology (BioLegend) and quantified on a Gallios cytofluorometer (Beckman Coulter).

Analysis of kidney involvement. Proteinuria was determined with semiquantitative urine testing strips (Albustix, Bayer) using midstream urine. For assessing glomerular immune and complement deposits, mice were perfused with PBS to minimize background. One kidney/mouse was embedded in OCT Tissue-Tek compound (Sakura), snap-frozen, and stored at –80°C. Cryosections (5 μm) were fixed with acetone and stained with FITC-labeled antibodies against murine IgG (BioLegend, catalog 405305) or complement factor C3 (Cedarlane, catalog CL7503F, clone RmC11H9). Deposits were scored by 2 blinded individual scorers by immunofluorescence microscopy on a Nikon Eclipse 80i microscope, utilizing a semiquantitative scoring system as described previously (4). The other kidney was fixed in Roti-Histofix (Carl Roth) and embedded in paraffin. The 5-μm sections were stained with periodic acid–Schiff (PAS) and then analyzed with a Zeiss AxioLab.A1 microscope and scored as described previously (10).

Measurement of ROS production. For measurement of intracellular ROS in mice and humans, lithium-heparinized blood was incubated with dihydrorhodamine 123 (3 μg/ml, Molecular Probes) for 15 minutes at 37°C. Cells were stained with either anti–mouse CD11b-eFluor450 (eBioscience, catalog 48-0112, clone M1/70), Ly6C-APC (Biolegend, catalog 128015, clone HK1.4), and Ly6G-PE/Cy7 (Biolegend catalog 127617, clone 1A8); or anti–human CD14-eFluor450 (eBioscience, catalog 48-0149, clone 61D3) and CD16-APC/Cy7 (Biolegend, catalog 302017, clone 3G8), and ROS production was induced by incubation with PMA (100 ng/ml) for 15 minutes at 37°C. Before analysis on the Beckman Coulter Gallios, samples were subjected to hypotonic water lysis. Detection of ROS released after in vitro treatment with RE-02 was performed as described previously (63).

Immunofluorescence staining of NETs. For detecting NETs in blood from mice and humans, 100 μl blood was incubated for 2 hours at 37°C with 100 ng/ml PMA or solvent or processed immediately. Erythrocytes were removed by hypotonic lysis. Cells were suspended in 1 ml PBS/1% paraformaldehyde. Cytospins were prepared, blocked with PBS/10% goat serum, and stained with either rabbit anti–histone H3 (Abcam, catalog ab131496) or rabbit anti–neutrophil elastase (anti-NE) (Abcam, catalog ab21595) in combination with a FITC-conjugated goat anti–rabbit IgG(H+L) detection antibody (Jackson ImmunoResearch, catalog 111-095-003). DNA was stained with propidium iodide (PI) (Sigma-Aldrich). Cytospins were analyzed on a BZ-X710 microscope (Keyence) and morphometric analysis was performed using Photoshop CS6 software. Percentage of NETs was defined as double-positive events with a 5-fold greater mean nuclear size of cells stained with PI and either citH3 or NE on 3 random slide sections.

For determination of pristane-induced NET formation, in vivo peritoneal lavages were collected 1 day after pristane injection. Cells were adjusted to 1×10^6 cells/ml. Cytospins were prepared, blocked with PBS/20% FCS, and incubated with rabbit anti–histone H3 (Abcam, catalog ab131496) or rabbit anti-NE (Abcam, catalog ab21595), and FITC-conjugated goat anti–rabbit IgG(H+L) (Jackson ImmunoResearch, catalog 111-095-003) for detection. DNA was stained with PI and cytospins were analyzed on a Nikon Eclipse 80i microscope. Percentage of NETs was defined as $PI^+/citH3^+$ events or PI^+/NE^+ events with a 5-fold greater mean nuclear size on 5 random slide sections.

The capacity of RE-02 to induce NET formation was determined on neutrophils isolated from thioglycollate-injected peritonea or human blood. Time-lapse videos were prepared on a BZ-X710 microscope (Keyence) after a 3-hour incubation of SYTOX Green Nucleic acid stain (Thermo Fisher)–dyed cells with various concentrations of RE-02, vehicle, or 100 ng/ml PMA in chamber slides. Quantification was performed on citH3- and NE-stained cells.

Statistics. Two-group comparisons were performed using 2-tailed Student's *t* test or, for non-normally distributed data by 2-tailed Mann-Whitney *U* test. Welch's correction was used in the case of unequal variances. Within each set of experiments shown in one figure multiple comparisons of groups were adjusted using Bonferroni's post-hoc test. Survival distributions during PIL were compared by Mantel-Cox test. Adjusted *P* values less than 0.05 were considered statistically significant. Levels of significance are labeled throughout the figures as follows: $*P < 0.05$, $**P < 0.01$, $***P < 0.001$. n.s. stands for not significant. Computations were performed and charts were produced using GraphPad Prism 5 software.

Study approval. All animal procedures were in accordance with institutional guidelines on animal welfare and were approved by the Semmelweis University Animal Experimentation Review Board (Budapest, Hungary), or the local ethical committee of the university Erlangen-Nuremberg, (Regierung von Mittelfranken, Würzburg, Germany).

All experiments including individuals with SLE and CGD and normal healthy donors were approved by the ethical committee of the university of Erlangen-Nuremberg, Erlangen, Germany. All persons enrolled in the study gave written informed consent.

Author contributions

DK and JH planned and performed most of the animal and in vitro experiments, conducted data analysis, helped write the manuscript, and prepared the figures. JS and TH planned and performed experiments with human samples. JZC and CR ran experiments with Mcl-$1^{\Delta Myelo}$ and control mice. VU provided samples and performed cytokine analysis. CJ, CM, MJP, and MB performed experiments with NOX2 inhibitors and conducted data analysis. ML, M. Hultqvist, PO, AM, M. Herrmann, GS, LEM, and RH provided scientific input, strategically planned the experiments, and helped write the manuscript. M. Hoffmann supervised the project, planned experiments, conducted data analysis, and wrote the manuscript. All authors read and approved the manuscript.

Acknowledgments

We thank Barbara Happich for technical assistance with histology and Kajsa Wing and Susann Winter for genotyping of *Ncf1*** mice.

This project was supported by the German Research Council (DFG CRC1181, project number C03), GK1660, the Städtler-Stiftung Nürnberg, the Swedish Strategic Science Foundation, the Knut and Alice Wallenberg foundation, the Swedish Research Council, the EU-projects RISE-Redoxit and Neurinox (Health-F2-2011-278611), and the Lendület program of the Hungarian Academy of Sciences (LP2013-66/2013 to AM). MaHo was further supported by the Austrian Science Fund (FWF, Project J3102-B13).

Address correspondence to: Markus H. Hoffmann, Universitätsstrasse 25a, 91054 Erlangen, Germany. Phone: 49.9131.8543024; E-mail: markus.hoffmann@uk-erlangen.de.

1. Baechler EC, et al. Interferon-inducible gene expression signature in peripheral blood cells of patients with severe lupus. *Proc Natl Acad Sci USA*. 2003;100(5):2610–2615.
2. Manderson AP, Botto M, Walport MJ. The role of complement in the development of systemic lupus erythematosus. *Annu Rev Immunol*. 2004;22:431–456.
3. Brinkmann V, et al. Neutrophil extracellular traps kill bacteria. *Science*. 2004;303(5663):1532–1535.
4. Kienhöfer D, et al. No evidence of pathogenic involvement of cathelicidins in patient cohorts and mouse models of lupus and arthritis. *PLoS One*. 2014;9(12):e115474.
5. Lande R, et al. Neutrophils activate plasmacytoid dendritic cells by releasing self-DNA-peptide complexes in systemic lupus erythematosus. *Sci Transl Med*. 2011;3(73):73ra19.
6. Hakkim A, et al. Impairment of neutrophil extracellular trap degradation is associated with lupus nephritis. *Proc Natl Acad Sci USA*. 2010;107(21):9813–9818.
7. Fuchs TA, et al. Novel cell death program leads to neutrophil extracellular traps. *J Cell Biol*. 2007;176(2):231–241.
8. Li P, Li M, Lindberg MR, Kennett MJ, Xiong N, Wang Y. PAD4 is essential for antibacterial innate immunity mediated by neutrophil extracellular traps. *J Exp Med*. 2010;207(9):1853–1862.
9. Kelkka T, et al. Reactive oxygen species deficiency induces autoimmunity with type 1 interferon signature. *Antioxid Redox Signal*. 2014;21(16):2231–2245.
10. Campbell AM, Kashgarian M, Shlomchik MJ. NADPH oxidase inhibits the pathogenesis of systemic lupus erythematosus. *Sci Transl Med*. 2012;4(157):157ra141.
11. Jacob CO, et al. Lupus-associated causal mutation in neutrophil cytosolic factor 2 (NCF2) brings unique insights to the structure and function of NADPH oxidase. *Proc Natl Acad Sci USA*. 2012;109(2):E59–E67.
12. De Ravin SS, et al. Chronic granulomatous disease as a risk factor for autoimmune disease. *J Allergy Clin Immunol*. 2008;122(6):1097–1103.
13. Satoh M, Reeves WH. Induction of lupus-associated autoantibodies in BALB/c mice by intraperitoneal injection of pristane. *J Exp Med*. 1994;180(6):2341–2346.
14. Nacionales DC, et al. Type I interferon production by tertiary lymphoid tissue developing in response to 2,6,10,14-tetramethylpentadecane (pristane). *Am J Pathol*. 2006;168(4):1227–1240.
15. Hochberg MC. Updating the American College of Rheumatology revised criteria for the classification of systemic lupus erythematosus. *Arthritis Rheum*. 1997;40(9):1725.
16. Reeves WH, Lee PY, Weinstein JS, Satoh M, Lu L. Induction of autoimmunity by pristane and other naturally occurring hydrocarbons. *Trends Immunol*. 2009;30(9):455–464.
17. Satoh M, et al. Widespread susceptibility among inbred mouse strains to the induction of lupus autoantibodies by pristane. *Clin Exp Immunol*. 2000;121(2):399–405.
18. Smith DL, Dong X, Du S, Oh M, Singh RR, Voskuhl RR. A female preponderance for chemically induced lupus in SJL/J mice. *Clin Immunol*. 2007;122(1):101–107.
19. Satoh M, Kumar A, Kanwar YS, Reeves WH. Anti-nuclear antibody production and immune-complex glomerulonephritis in BALB/c mice treated with pristane. *Proc Natl Acad Sci USA*. 1995;92(24):10934–10938.
20. Chowdhary VR, Grande JP, Luthra HS, David CS. Characterization of haemorrhagic pulmonary capillaritis: another manifestation of Pristane-induced lupus. *Rheumatology (Oxford)*. 2007;46(9):1405–1410.
21. Kamen DL, Strange C. Pulmonary manifestations of systemic lupus erythematosus. *Clin Chest Med*. 2010;31(3):479–488.
22. Calvani N, et al. Induction of apoptosis by the hydrocarbon oil pristane: implications for pristane-induced lupus. *J Immunol*. 2005;175(7):4777–4782.
23. Herman S, et al. Cell death and cytokine production induced by autoimmunogenic hydrocarbon oils. *Autoimmunity*. 2012;45(8):602–611.
24. Dahlgren J, Takhar H, Anderson-Mahoney P, Kotlerman J, Tarr J, Warshaw R. Cluster of systemic lupus erythematosus (SLE) associated with an oil field waste site: a cross sectional study. *Environ Health*. 2007;6:8.
25. Dzhagalov I, St John A, He YW. The antiapoptotic protein Mcl-1 is essential for the survival of neutrophils but not macrophages. *Blood*. 2007;109(4):1620–1626.
26. Calvani N, Satoh M, Croker BP, Reeves WH, Richards HB. Nephritogenic autoantibodies but absence of nephritis in Il-12p35-deficient mice with pristane-induced lupus. *Kidney Int*. 2003;64(3):897–905.
27. Lee PY, et al. A novel type I IFN-producing cell subset in murine lupus. *J Immunol*. 2008;180(7):5101–5108.

28. Wang Y, et al. Histone hypercitrullination mediates chromatin decondensation and neutrophil extracellular trap formation. *J Cell Biol*. 2009;184(2):205–213.
29. Neeli I, Radic M. Opposition between PKC isoforms regulates histone deimination and neutrophil extracellular chromatin release. *Front Immunol*. 2013;4:38.
30. Schauer C, et al. Aggregated neutrophil extracellular traps limit inflammation by degrading cytokines and chemokines. *Nat Med*. 2014;20(5):511–517.
31. Gresnigt MS, et al. Neutrophil-mediated inhibition of proinflammatory cytokine responses. *J Immunol*. 2012;189(10):4806–4815.
32. Villanueva E, et al. Netting neutrophils induce endothelial damage, infiltrate tissues, and expose immunostimulatory molecules in systemic lupus erythematosus. *J Immunol*. 2011;187(1):538–552.
33. Bennett L, et al. Interferon and granulopoiesis signatures in systemic lupus erythematosus blood. *J Exp Med*. 2003;197(6):711–723.
34. Carmona-Rivera C, Kaplan MJ. Low-density granulocytes: a distinct class of neutrophils in systemic autoimmunity. *Semin Immunopathol*. 2013;35(4):455–463.
35. Lood C, et al. Neutrophil extracellular traps enriched in oxidized mitochondrial DNA are interferogenic and contribute to lupus-like disease. *Nat Med*. 2016;22(2):146–153.
36. Tan EM, et al. The 1982 revised criteria for the classification of systemic lupus erythematosus. *Arthritis Rheum*. 1982;25(11):1271–1277.
37. Bengtsson AA, et al. Low production of reactive oxygen species in granulocytes is associated with organ damage in systemic lupus erythematosus. *Arthritis Res Ther*. 2014;16(3):R120.
38. Smith CK, Kaplan MJ. The role of neutrophils in the pathogenesis of systemic lupus erythematosus. *Curr Opin Rheumatol*. 2015;27(5):448–453.
39. Knight JS, et al. Peptidylarginine deiminase inhibition is immunomodulatory and vasculoprotective in murine lupus. *J Clin Invest*. 2013;123(7):2981–2993.
40. Chumanevich AA, et al. Suppression of colitis in mice by Cl-amidine: a novel peptidylarginine deiminase inhibitor. *Am J Physiol Gastrointest Liver Physiol*. 2011;300(6):G929–G938.
41. Knight JS, et al. Peptidylarginine deiminase inhibition reduces vascular damage and modulates innate immune responses in murine models of atherosclerosis. *Circ Res*. 2014;114(6):947–956.
42. Wei L, Wasilewski E, Chakka SK, Bello AM, Moscarello MA, Kotra LP. Novel inhibitors of protein arginine deiminase with potential activity in multiple sclerosis animal model. *J Med Chem*. 2013;56(4):1715–1722.
43. Nauseef WM. Assembly of the phagocyte NADPH oxidase. *Histochem Cell Biol*. 2004;122(4):277–291.
44. Olofsson P, Holmberg J, Tordsson J, Lu S, Akerström B, Holmdahl R. Positional identification of Ncf1 as a gene that regulates arthritis severity in rats. *Nat Genet*. 2003;33(1):25–32.
45. Hultqvist M, Olofsson P, Holmberg J, Bäckström BT, Tordsson J, Holmdahl R. Enhanced autoimmunity, arthritis, and encephalomyelitis in mice with a reduced oxidative burst due to a mutation in the Ncf1 gene. *Proc Natl Acad Sci USA*. 2004;101(34):12646–12651.
46. Khmaladze Ia, et al. Mannan induces ROS-regulated, IL-17A-dependent psoriasis arthritis-like disease in mice. *Proc Natl Acad Sci USA*. 2014;111(35):E3669–E3678.
47. Mossberg N, et al. Oxygen radical production and severity of the Guillain--Barré syndrome. *J Neuroimmunol*. 2007;192(1–2):186–191.
48. van de Loo FA, et al. Deficiency of NADPH oxidase components p47phox and gp91phox caused granulomatous synovitis and increased connective tissue destruction in experimental arthritis models. *Am J Pathol*. 2003;163(4):1525–1537.
49. Whitmore LC, Goss KL, Newell EA, Hilkin BM, Hook JS, Moreland JG. NOX2 protects against progressive lung injury and multiple organ dysfunction syndrome. *Am J Physiol Lung Cell Mol Physiol*. 2014;307(1):L71–L82.
50. Noack D, et al. Autosomal recessive chronic granulomatous disease caused by defects in NCF-1, the gene encoding the phagocyte p47-phox: mutations not arising in the NCF-1 pseudogenes. *Blood*. 2001;97(1):305–311.
51. Urbonaviciute V, et al. Toll-like receptor 2 is required for autoantibody production and development of renal disease in pristane-induced lupus. *Arthritis Rheum*. 2013;65(6):1612–1623.
52. Kavanaugh A, Tomar R, Reveille J, Solomon DH, Homburger HA. Guidelines for clinical use of the antinuclear antibody test and tests for specific autoantibodies to nuclear antigens. American College of Pathologists. *Arch Pathol Lab Med*. 2000;124(1):71–81.
53. Cortés-Hernández J, et al. Antihistone and anti-double-stranded deoxyribonucleic acid antibodies are associated with renal disease in systemic lupus erythematosus. *Am J Med*. 2004;116(3):165–173.
54. Migliorini P, Baldini C, Rocchi V, Bombardieri S. Anti-Sm and anti-RNP antibodies. *Autoimmunity*. 2005;38(1):47–54.
55. Holmdahl R, Sareila O, Olsson LM, Bäckdahl L, Wing K. Ncf1 polymorphism reveals oxidative regulation of autoimmune chronic inflammation. *Immunol Rev*. 2016;269(1):228–247.
56. Yousefi S, Simon HU. NETosis - does it really represent nature's "suicide bomber"? *Front Immunol*. 2016;7:328.
57. Konig MF, Andrade F. A critical reappraisal of neutrophil extracellular traps and NETosis mimics based on differential requirements for protein citrullination. *Front Immunol*. 2016;7:461.
58. Yipp BG, Kubes P. NETosis: how vital is it? *Blood*. 2013;122(16):2784–2794.
59. Hultqvist M, Olofsson P, Wallner FK, Holmdahl R. Pharmacological potential of NOX2 agonists in inflammatory conditions. *Antioxid Redox Signal*. 2015;23(5):446–459.
60. Reinwald C, et al. Reply to "Neutrophils are not required for resolution of acute gouty arthritis in mice". *Nat Med*. 2016;22(12):1384–1386.
61. Huang CK, Zhan L, Hannigan MO, Ai Y, Leto TL. P47(phox)-deficient NADPH oxidase defect in neutrophils of diabetic mouse strains, C57BL/6J-m db/db and db/+. *J Leukoc Biol*. 2000;67(2):210–215.
62. Sareila O, Jaakkola N, Olofsson P, Kelkka T, Holmdahl R. Identification of a region in p47phox/NCF1 crucial for phagocytic NADPH oxidase (NOX2) activation. *J Leukoc Biol*. 2013;93(3):427–435.
63. Lundqvist H, Dahlgren C. Isoluminol-enhanced chemiluminescence: a sensitive method to study the release of superoxide anion from human neutrophils. *Free Radic Biol Med*. 1996;20(6):785–792.